Effects of Small-Scale Heterogeneities on Regional Propagation

S. Flatté

March 1990

JSR-89-151

JASON
The MITRE Corporation
7525 Colshire Drive
McLean, Virginia 22102-3481
(703) 883-6997

SECURITY CLASSIFICATION OF THIS PAGE

REPORT DOCUMENTATION PAGE

Form Approved
OMB No 0704-0188
Exp. Date Jun 30, 1986

1a REPORT SECURITY CLASSIFICATION UNCLASSIFIED	1b RESTRICTIVE MARKINGS NONE
2a SECURITY CLASSIFICATION AUTHORITY N/A SINCE UNCLASSIFIED 2b DECLASSIFICATION/DOWNGRADING SCHEDULE N/A SINCE UNCLASSIFIED	3 DISTRIBUTION/AVAILABILITY OF REPORT Approved for public release; distribution unlimited.
4 PERFORMING ORGANIZATION REPORT NUMBER(S) JSR-89-151	5 MONITORING ORGANIZATION REPORT NUMBER(S) JSR-89-151
6a NAME OF PERFORMING ORGANIZATION JASON Program Office The MITRE Corporation 6b OFFICE SYMBOL (If applicable) A10	7a NAME OF MONITORING ORGANIZATION DARPA
6c ADDRESS (City, State, and ZIP Code) 7525 Colshire Drive McLean, VA 22102-3481	7b ADDRESS (City, State, and ZIP Code) 1400 Wilson Boulevard Arlington, VA 22209-2308
8a NAME OF FUNDING/SPONSORING ORGANIZATION DARPA 8b OFFICE SYMBOL (If applicable) TIO	9 PROCUREMENT INSTRUMENT IDENTIFICATION NUMBER
8c ADDRESS (City, State, and ZIP Code) 1400 Wilson Boulevard Arlington, VA 22209-2308	10 SOURCE OF FUNDING NUMBERS PROGRAM ELEMENT NO: PROJECT NO: 8503Z TASK NO: WORK UNIT ACCESSION NO:

11 TITLE (Include Security Classification)
Effects of Small Scale Heterogeneities on Regional Propagation

12 PERSONAL AUTHOR(S)
Stanley M. Flatte

13a TYPE OF REPORT	13b TIME COVERED	14 DATE OF REPORT (Year, Month, Day)	15 PAGE COUNT
Technical	FROM ______ TO ______	90/01/21	25

16 SUPPLEMENTARY NOTATION

17 COSATI CODES		
FIELD	GROUP	SUB-GROUP

18 SUBJECT TERMS (Continue on reverse if necessary and identify by block number)
propagation; heterogeneities; seismic-wave, crustal waveguide.

19 ABSTRACT (Continue on reverse if necessary and identify by block number)

Regional seismic-wave propagation at frequencies above 1 Hz is described in terms of ray theory, and the effects of small-scale heterogeneities are described statistically by means of the modern theory of wave propagation through random media. Observed features of regional propagation, such as the complexity of waveforms over tens or hundreds of seconds, the sensitivity of this complexity to the location of source or receiver, and the spread in arrival angles of waves at a receiving array, are explained by this propagation model.

20 DISTRIBUTION/AVAILABILITY OF ABSTRACT ☒ UNCLASSIFIED/UNLIMITED ☐ SAME AS RPT ☐ DTIC USERS	21 ABSTRACT SECURITY CLASSIFICATION UNCLASSIFIED
22a NAME OF RESPONSIBLE INDIVIDUAL Dr. Robert G. Henderson	22b TELEPHONE (Include Area Code) (703) 883-6997 22c OFFICE SYMBOL JASON Prog Ofc

DD FORM 1473, 84 MAR — 83 APR edition may be used until exhausted. All other editions are obsolete.

SECURITY CLASSIFICATION OF THIS PAGE

Abstract

Regional seismic-wave propagation at frequencies above 1 Hz is described in terms of ray theory, and the effects of small-scale heterogeneities are described statistically by means of the modern theory of wave propagation through random media. Observed features of regional propagation, such as the complexity of waveforms over tens or hundreds of seconds, the sensitivity of this complexity to the location of source or receiver, and the spread in arrival angles of waves at a receiving array, are explained by this propagation model.

Contents

1 INTRODUCTION

Seismic waves travelling over regional distances (100-1000 km) from shallow sources must travel through the crustal waveguide. There have been many studies of this type of propagation, and a number of attempts to explain its behavior in terms of models of earth structure. Some explanations have concentrated on the details of horizontally stratified wavespeed structure, with the wave equation being solved in terms of normal modes.[1] Other explanations have used ray theory as a starting point.[2] Most of these analyses have modelled earth structure in a deterministic manner; that is, models were presented that defined the seismic wavespeed exactly for every point in space.

For seismic waves above 1 Hz, a number of recent studies have analysed waveform variability in terms of a statistical model of earth heterogeneities. Teleseismic P-wave amplitude and arrival-time fluctuations have been explained on the basis of heterogeneities in the lithosphere and upper mantle; these studies were sensitive to heterogeneities with rms wavespeed variations of a few percent and horizontal scale lengths from a few kilometers to tens of kilometers.[3] These teleseismic waves come up toward the receiver stations with angles not to far from the zenith. (See Figure 1.) Propagation over regional distances from deep earthquakes (well below the crust) has also been analysed in terms of heterogeneities, and similar results have been obtained.[4]

In both the above studies, the model of deterministic propagation, before the addition of heterogeneities, was a very simple one; it consisted of incident straight-line rays, or plane waves.

It is the purpose of this study to analyse regional propagation from shallow sources from the same point of view as the above studies. For this purpose we must make a simple model of deterministic propagation in the absence of heterogeneities; this is done in Section 2. Then the effects of heterogeneities are added in Section 3. We will see that this statistical approach explains many of the features of regional propagation.

Our simple model consists of a constant-depth crustal waveguide with a constant wavespeed, overlying a uniform half-space with a constant (higher)

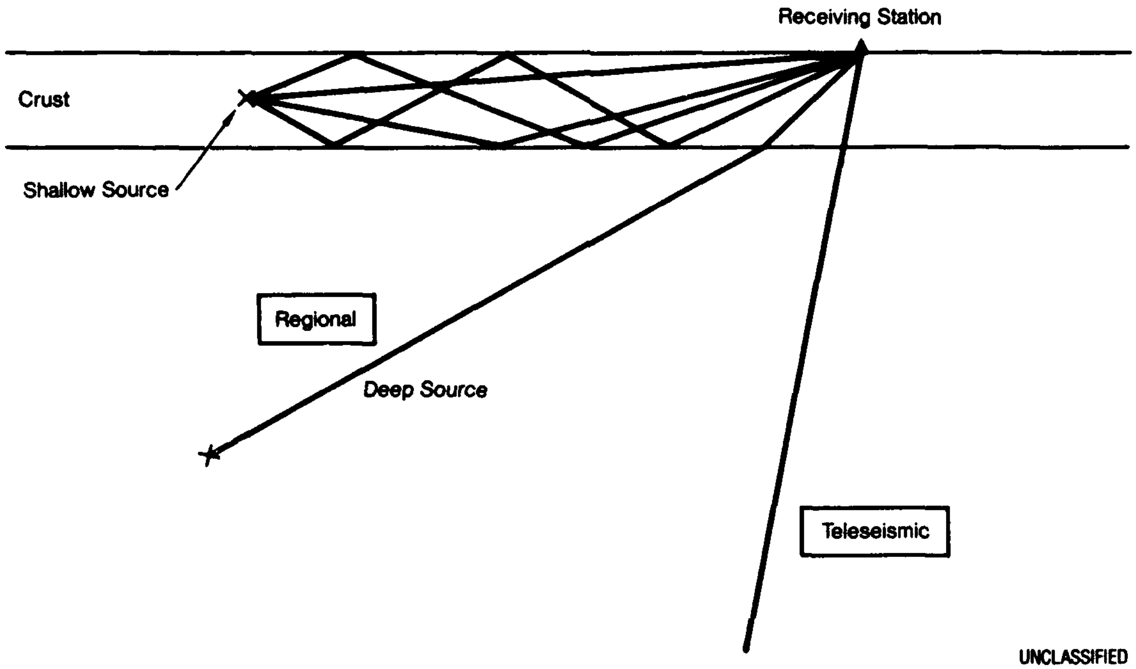

Figure 1. Schematic of the arrival of seismic waves at a receiver on the earth's surface, for a simple deterministic model of earth structure involving the crustal waveguide. Waves from near the zenith come nearly straight through; they represent teleseismic arrivals. Waves from sources that are below the crustal waveguide are refracted slightly, but still have a single, well-defined ray as a deterministic model of the propagation. Waves from sources within the crustal waveguide can reflect many times on their way to a receiver.

wavespeed. A real region of the crust will be more complicated than our simple model, even disregarding small-scale heterogeneities. For example, the depth of the waveguide may be variable with geographical position, or the wavespeed may have a small gradient, or a series of step changes within the waveguide. We will see that when we add the heterogeneities, the complexity introduced into the received waveforms is so drastic, that if we had started with a more complicated deterministic model, it would not have qualitatively changed our conclusions.

In this study we will ignore the problem of conversion between compressional and shear waves. Our study may be thought of as initially applying to SH propagation, since there is no conversion of SH waves in our deterministic model. Again, the variations introduced by the heterogeneities are so significant, even for pure SH waves, that our qualitative conclusions will probably apply in general, but this is clearly an area deserving of further first-order study.

2 CRUSTAL WAVEGUIDE PROPAGATION

Deterministic propagation in the crustal waveguide at high frequencies can be analysed from the point of view of ray theory. Our model will be a uniform-speed waveguide of thickness h and wavespeed β, with a uniform-speed half-space underlying it. The speed in the underlying medium will be designated β_2. We will take a source at depth d at a distance R from a receiver station on the surface. (See Figure 2.)

The solution to our simple model is straightforward, and consists of a sequence of straight-line rays that are reflected n times from the surface or bottom of the waveguide, where n is 0, ± 1, ± 2 ... up to a maximum determined by critical reflection at the bottom of the waveguide. This critical reflection angle is determined by the ratio of the wavespeeds in the two regions of the earth:

$$\cos\Theta_{\text{critical}} < \beta/\beta_2.$$

Let Θ_n be the angle of the nth ray with the horizontal. The requirement that $\Theta_n < \Theta_{\text{critical}}$ can be more usefully expressed by the equation:

$$|d + 2nh| < \left[(\beta_2/\beta)^2 - 1\right]^{1/2} R.$$

The number of rays N can be expressed approximately from this equation:

$$N = (R/h)\left[(\beta_2/\beta)^2 - 1\right]^{1/2}.$$

The intensity of each ray can be calculated from simple spherical spreading, because each ray can be unwrapped from its reflections into a simple straight line having a length of $R/cos\Theta_n$. Therefore, the intensity of the nth ray is:

$$I_n = S(\Theta_n)cos^2\Theta_n/R^2 = S(\Theta_n)/[R^2 + (d + 2nh)^2]$$

where $S(\Theta_n)$ is the angular distribution at the source. From here on we will assume for simplicity that the source is isotropic; that is, $S(\Theta_n) = 1$. If we normalize the intensity pattern by having the first ray (with n=0) have

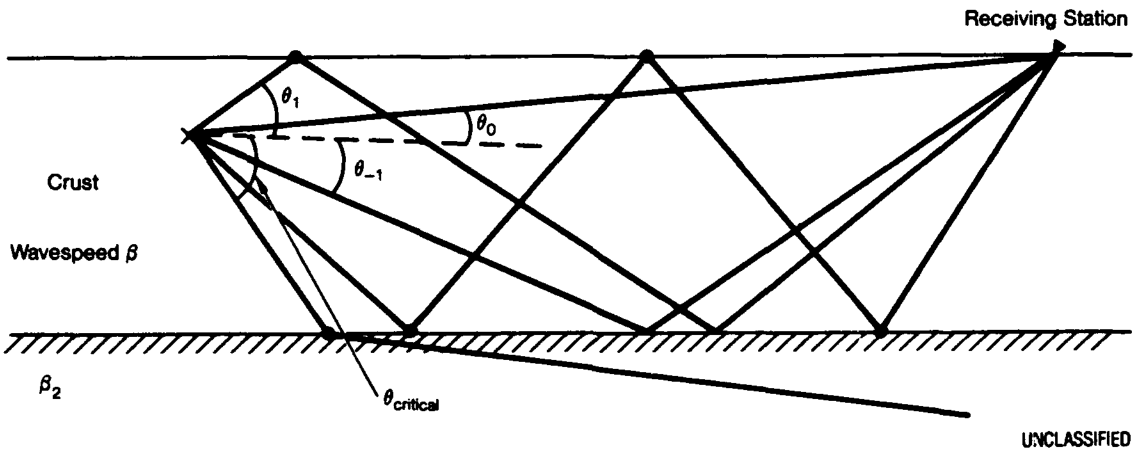

Figure 2. Diagram of rays from a source in the crustal waveguide to a receiver on the surface. Each ray has an angle θ_n with the horizontal. The wavespeeds in the crustal waveguide and below are β and β_2, respectively. Rays with angles above the critical angle get lost in the deep earth.

an intensity of unity, then it is easy to show that the last ray will have the minimum intensity, and it will be

$$I_{\text{min}} = (\beta/\beta_2)^2$$

The arrival time of each ray is easily calculated from the distance travelled $(R/cos\Theta_n)$:

$$t_n = (R/\beta)\left\{1 + [(d + 2nh)/R]^2\right\}^{1/2}.$$

Note that if $d << h$, then the two rays corresponding to positive and negative n come in very close together; there is a twinning of arrivals associated with the source and its image reflected in the earth's surface. The patterns that result for several ranges of propagation in a crustal waveguide with realistic average values for the various characteristic parameters are shown in Figure 3.

It is useful to calculate the approximate spacing between the discrete arrivals for later comparison with the effects of heterogeneities. Let Δt_n be the spacing between the nth and (n+1)th rays:

$$\Delta t_n = (2h/\beta)\xi_n/[1 + \xi_n^2]^{1/2}$$

where

$$\xi_n = |(d + 2nh)/R|.$$

This expression does not account for the twinning due to positive and negative n. It is of interest to note that near the first arrival, the separation is much smaller than near the last arrival:

$$\begin{aligned} \Delta t_1 &= (2h/\beta)(2h/R) \\ \Delta t_{\text{max}} &= (2h/\beta). \end{aligned}$$

For example, if h=30 km, R=600 km, and β =3 km/s, then $\Delta t_1 = 2$ s and $\Delta t_{\text{max}} = 20$ s.

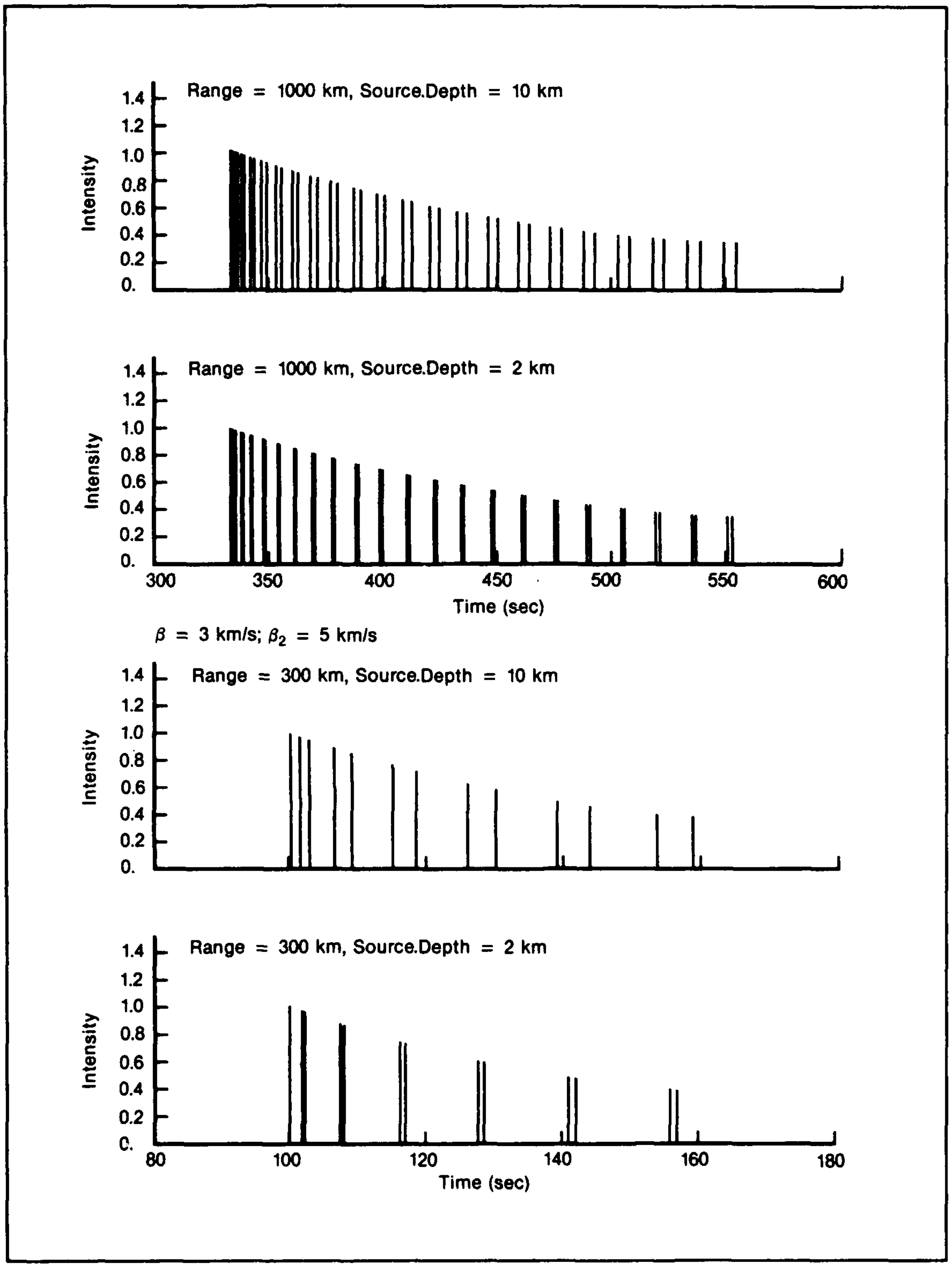

UNCLASSIFIED

Figure 3. (U) Examples of expected high-frequency waveforms for our simple deterministic crustal waveguide parameters, with no heterogeneities. The plots are for two different ranges (300 km and 1000 km) and two different source depths (2 km and 10 km). The parameters of the crust are: h=30 km, β=3 km/s, and β_2=5 km/s.

3 THE EFFECTS OF HETEROGENEITIES

The simple arrival structure described in Section 2 is not observed experimentally. The arrival pattern is more complex, with intensity as a function of time being an apparently random jumble that begins about where the first arrival is expected, and continues until dying away in the noise many tens of seconds later.

We will calculate the effect of small-scale heterogeneities on our deterministic arrival structure by use of the path-integral theory of wave propagation through random media, developed in large part for the case of acoustic propagation in the ocean.[5-11] To begin with, we need a statistical model for the heterogeneities. For the purpose of this illustrative study, we will take an anisotropic Gaussian correlation function with scale lengths in the horizontal (L_V) and vertical (L_H) and an rms fractional variation in wavespeed of μ.

We emphasize that we are taking a simplistic picture of the medium in assuming that it is composed of the superposition of two disparate structures: First, a very simple deterministic structure (a plane layer over a homogeneous half-space), and second, small-scale random velocity perturbations in the crustal layer. Other effects, which are certainly of importance in specific regions, might be topography on the surfaces of the crustal layer, or reflecting surfaces within the crust. The point of our study is that much of what is actually observed may often be explained by random volume velocity perturbations, so that such perturbations should not be ignored in a first-order explanation of observations, particularly at high frequency.

We will take the values of velocity-fluctuation quantities from the studies that have been carried out on teleseismic waves arriving at large arrays, and from recent studies of regional propagation from deep earthquakes. The relation between crustal-waveguide propagation and teleseismic effects is dependent on the anisotropy of the medium fluctuations, which is not well known. We are only giving order-of-magnitude examples here; in the study of a specific geographical region, careful consideration to specific anisotropy models should be given.

Typical values of these fluctuation quantities, from the teleseismic study and the study of regional propagation from deep earthquakes, might be: $\mu \sim 2\%$, $L_V \sim 5$ km, and $L_H \sim 10$ km. However, the results are quite sensitive to the exact choices of values, and to the particular spectrum chosen. Therefore, a more quantitative study must be done to compare with actual data from a specific geographical region.

3.1 Fluctuation Regime

Various regimes of wave fluctuation behavior were identified in Reference 5 and 6, and quantities were defined that are necessary for determining the regime in which a particular situation lies. These quantities are:

- The strength parameter Φ, which is the rms phase that a wave would experience if it travelled exactly along the deterministic ray. This would be the actual rms phase only if the heterogeneities were weak enough, but even when the heterogeneities are strong, the calculation of the strength parameter is crucial to the wave-fluctuation analysis.
- The diffraction parameter Λ, which is the square of the ratio between the size of the Fresnel zone and the transverse correlation length of the medium, averaged over the deterministic ray. Small diffraction parameter means that diffraction is small, so that the concepts of generalized geometrical optics are quite useful. Large diffraction parameter means that diffraction is very important; in this situation concepts of uncorrelated multiple scatter are probably useful.
- The various regimes in $\Lambda - \Phi$ space are shown in Figure 4. We need to define a few more quantities in order to calculate these parameters. They are:
- The wavenumber of the propagating seismic wave, which we will denote by q. For example, a 1-Hz shear wave travelling in a crust with a speed of 3.14 km/s has a wavenumber q = 2 km^{-1}.

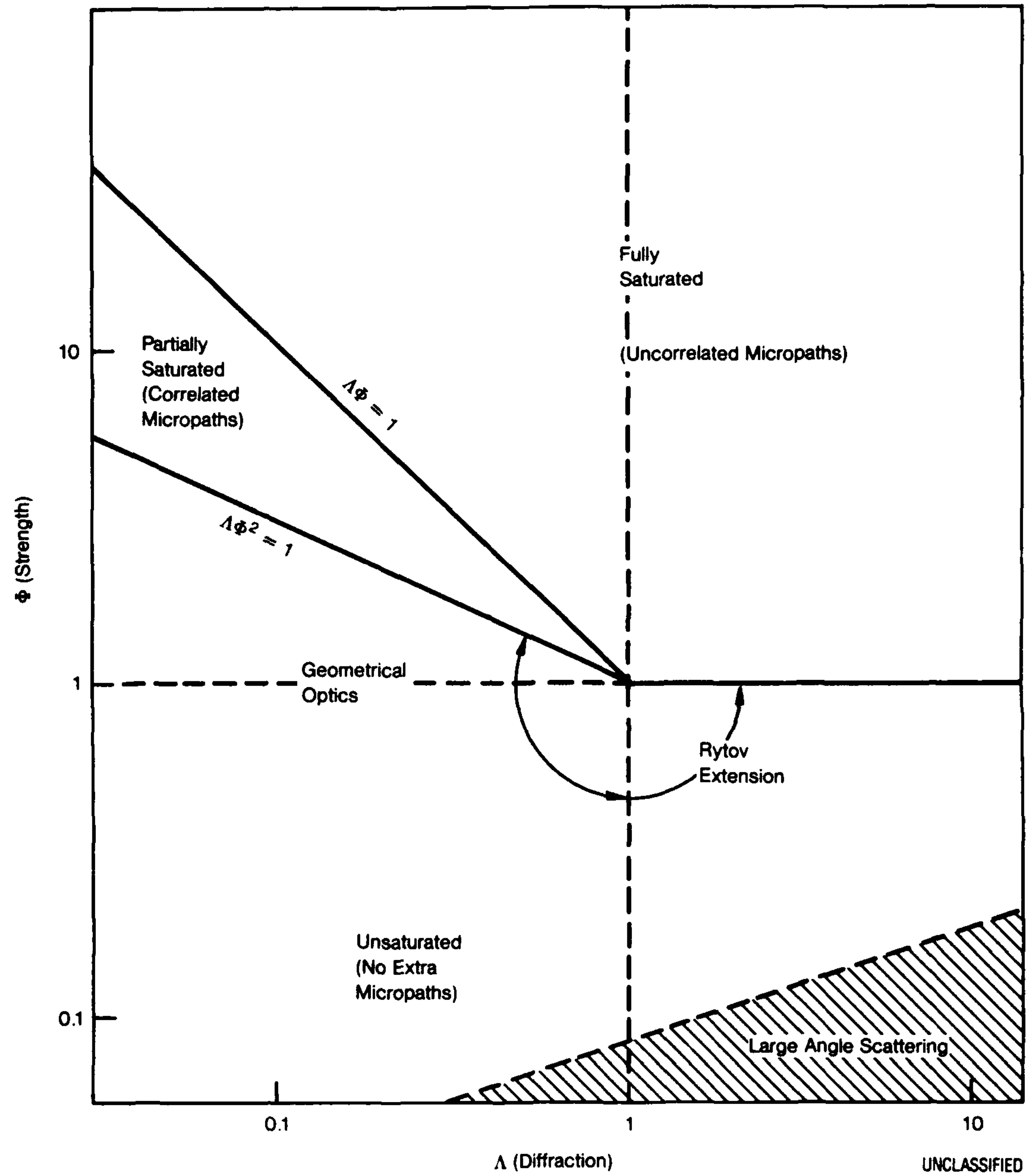

Figure 4. Λ–Φ diagram showing the different regimes of wave fluctuation behavior for waves propagating through random media (from Reference 6).

- The parallel (L_P) and transverse (L_T) correlation length of the medium, where parallel means along the deterministic ray, and transverse means perpendicular to the deterministic ray. In an anisotropic medium, these can often be expressed in terms of L_V and L_H.

In terms of defined quantities, the following results for the strength and diffraction parameters follow:

$$\begin{aligned}
\Phi^2 &= q^2\mu^2 L_P R = 16 \\
\Lambda &= R/(6qL_T^2) = 3.3 \\
\Lambda\Phi^2 &= (1/6)q\mu^2 R^2 L_P/L_T^2 = 53 \\
\Lambda\Phi &= (1/6)\mu R(L_P R)^{1/2}/L_T^2 = 13
\end{aligned}$$

and putting in our so-called typical numbers yields the numerical values indicated, for a propagation range of 1000 km.

The fact that both $\Lambda\Phi$ and Φ are greater than unity tells us that we are in full saturation. In this regime we have many uncorrelated microrays; that is, each deterministic ray is broken up by the heterogeneities into many rays. This remains true as one moves to higher frequency.

3.2 Intensity Fluctuations

In the fully saturated regime, the intensity of a given ray, at least at a single frequency, is Rayleigh distributed. That means that the intensity has a simple exponential distribution function. As long as the analysis is being done on a limited frequency band that does not exceed the coherent bandwidth, the result is that each of the arrivals in, for example, Figure 3, will have an intensity taken from this exponential distribution function, with mean value given by the deterministic result. However, as will be shown below, the case of interest here has a very small coherent bandwidth. In that case, the observation can be thought of as being within a small interval of time, so small that the time spread of the received pulse is much larger than the observation interval, and the intensity within each observation time interval will be a random variable with a large variance.

3.3 Time Spread

In the fully saturated regime, a delta-function pulse emitted by the source is spread in time by an amount given by[5]

$$\tau_n = \Lambda\Phi^2/(q\beta)\left\{1 + \xi_n^2\right\}.$$

We can compare this spread to the separation between the deterministic arrivals by taking the ratio of the two:

$$\tau_n/\Delta t_n = \Lambda\Phi^2/(2qh)[1 + \xi_n^2]^{3/2}/\xi_n.$$

The ξ_n at small n are small compared with unity (on the order of h/R), and rise to a maximum of

$$\xi\text{max} = \left[(\beta_2/\beta)^2 - 1\right]^{1/2}.$$

A few simple substitutions of numerical values reveals that the ratio of $\tau/\Delta t$ is always greater than unity. Thus the spread due to heterogeneities is always larger than the separation between deterministic arrivals, resulting in a waveform that essentially appears to be random.

For example, for our typical numbers at 1000 km range, we find that

$$\begin{aligned}\tau_1 &= 9s\\ \tau_N &= 25s\end{aligned}$$

and we see that in all cases the spread fills in any gaps one might have observed in the deterministic propagation.

The coherent bandwidth of the propagation is the inverse of the time spread. The numbers above imply that the coherent bandwidth is in the range of 0.04-0.10 Hz.

3.4 Angular Spread

In the fully saturated regime, the energy that starts from a point source and arrives at a point receiver has travelled within a spatial region that is determined by the medium fluctuations rather than the finite wavelength of the seismic wave. The size of this spatial region also determines the spread in arrival angle of the energy as it arrives at the receiver.

The determination of this angular spread is dependent on a function known as the phase structure function, which is the variance of phase difference between two nearby rays that start from the source and end near the receiver with a small separation x. In the case of a Gaussian correlation function, the phase structure function D is given by

$$D(x) = \Phi^2 (x/L_T)^2.$$

The rms angular spread is determined by the value of x (call it x_o) at which $D(x_o)=1$. Thus:

$$x_o = L_T/\Phi$$

and

$$\Theta_{\text{rms}} = 1/(x_o q) = \Phi/(qL_t).$$

For our typical case, in which $\Phi = 4, q = 2$ km^{-1}, and $L_T = 5$ km, we have $\Theta_{\text{rms}} = 0.4$ radians, or 23°. Note that the angular spread scales with the square root of range, and is independent of frequency.

Thus, an array that attempts to determine the location of the source by beamforming will find that the inherent inaccuracy due to the heterogeneities has a standard deviation on the order of 20° at 1000 km.

3.5 Averaging and Calibration Distances

The distance x_o represents the distance over which the arriving wave field is decorrelated. Therefore, if one wants to go back and verify the exact waveform received in a particular event by repeating the transmission by some means, then one must place both the source and the receiver within a fraction of x_o of the original transmission. This would be true for both the horizontal and vertical position. In our typical case, the value of x_o is about 1 km.

By the same token, if one were attempting to average out the effects of heterogeneities, one would get approximately independent samples every x_o, and therefore many receivers spaced by that distance would give a good average.

However, this conclusion is really not accurate for media that are multiscale rather than Gaussian. We would expect that the larger averaging region would be affected by larger-scale medium variations, and the variance would not go down proportionally to the number of receiving stations. This kind of calculation can be done for any given model of medium fluctuations.

4 DISCUSSION AND CONCLUSIONS

An intuitive understanding of regional propagation of high frequency seismic waves for sources that lie within the crustal waveguide has been presented in terms of a very simple deterministic propagation model combined with the effects of small-scale heterogeneities. Our simple deterministic model implies that the underlying pattern of arrivals is a series of sharp arrivals associated with the multiray structure expected in a waveguide. Reasonable numerical values for heterogeneities in the crust yield very significant effects on the received arrivals. These effects include variations in amplitude, arrival time, and arrival angle. As a result of these fluctuations, the received waveforms will lose their detailed connection with the underlying arrival pattern, and will become a jumble of arrivals whose spread in time overlaps with the nearby deterministic arrivals. The variations in intensity of each arrival caused by the heterogeneities are large.

The angular spread of the arriving energy can be calculated, and for 1000-km propagation has an rms value of 20° or more. This angular spread also implies that nearby receivers will not be coherent with each other at distances comparable to 1 km, and that the use of calibration shots of some kind in order to measure the propagation from a particular source to a particular receiver must be done under the limitation that the calibration shot must be within that 1-km distance.

REFERENCES

1. B.L.N. Kennett, Lg-Wave Propagation in Heterogeneous Media, Final Report, 15 Feb. 1988-14 Feb. 1989, GL-TR-89-0102.

2. R.W. Clayton, D.G. Harkrider, and D.V. Helmberger, Modeling Regional Seismic Waves from Underground Nuclear Explosion, Scientific Report No. 1, 9 May, 1988, AFGL-TR-88-0135.

3. S.M. Flatté and R.S. Wu, J. Geophys. Res. 93, 6601 (1988).

4. H. Sato, Broadening of Seismogram Envelopes in the Randomly Inhomogeneous Lithosphere Based on the Parabolic Approximation: Southeaster Honshu, Japan, J. Geophys. Res., in press (1989).

5. S.M. Flatté et al, Sound Transmission through a Fluctuating Ocean, Cambridge University Press, New York (1979).

6. S.M. Flatté, PROC. IEEE, 71, 1267-1294 (1983).

7. R. Dashen, S.M. Flatté, and S.A. Reynolds, J. Acoust. Soc. Am. 77, 1718 (1985).

8. S.A. Reynolds et al, J. Acoust. Soc. Am. 77, 1723 (1985).

9. S.M. Flatté, S.A. Reynolds, and R. Dashen, J. Acoust. Soc. Am. 82, 967 (1987).

10. S.M. Flatté et al, J. Acoust. Soc. Am. 82, 973 (1987).

11. S.M. Flatté and R. Stoughton, J. Acoust. Soc. Am. 84, 1414 (1988).

DISTRIBUTION LIST

Dr. Henry D.I. Abarbanel
Institute for Nonlinear Science
Mail Code R002/Building CMRR/Room 115
University of California/San Diego
La Jolla, CA 92093-0402

Dr. Ralph W. Alewine III
Director
Nuclear Monitoring Research Office
DARPA/NMRO
1400 Wilson Boulevard
Arlington, VA 22209-2308

Dr. Marvin C. Atkins [3]
Deputy Director
Science and Technology
Defense Nuclear Agency
6801 Telegraph Road
Alexandria, VA 22310

The Honorable John A. Betti
Undersecretary of Defense for Acquisition
The Pentagon, Room 3E933
Washington, DC 20301-3000

Dr. Arthur E. Bisson
Technical Director of Submarine
and SSBN Security Program
Department of the Navy, OP-02T
The Pentagon, Room 4D534
Washington, DC 20350-2000

Dr. Robert R. Blandford
DARPA/NMRO
1400 Wilson Boulevard
Arlington, VA 22209-2308

Mr. Edward C. Brady
Sr. Vice President and General Manager
The MITRE Corporation
Mail Stop Z605
7525 Colshire Drive
McLean, VA 22102

The Honorable D. Allan Bromley
Asst to the President for Science and
Technology
Office of Science and Technology Policy
Old Executive Office Building, Room 360
17th & Pennsylvania Avenue, N.W.
Washington, DC 20506

Mr. Edward Brown
DARPA/PM
1400 Wilson Boulevard
Arlington, VA 22209-2308

Dr. Herbert L. Buchanan, III
Director
DARPA/DSO
1400 Wilson Boulevard
Arlington, VA 22209-2308

Dr. Kenneth M. Case
Institute for Nonlinear Science
Mail Code R-002
University of California/San Diego
San Diego, CA 92093-0402

Dr. Ferdinand N. Cirillo, Jr.
Central Intelligence Agency
Washington, DC 20505

DISTRIBUTION LIST

Mr. John Darrah
Senior Scientist and Technical Advisor
HQAF SPACOM/CN
Peterson AFB, CO 80914-5001

Dr. Russ E. Davis
Scripps Institution of Oceanography
A-030
University of California/San Diego
La Jolla, CA 92093

DTIC [2]
Defense Technical Information Center
Cameron Station
Alexandria, VA 22314

Professor Freeman J. Dyson
Institute for Advanced Study
Olden Lane
Princeton, NJ 08540

Maj Gen Robert D. Eaglet
Assistant Deputy SAF/AQ
The Pentagon, Room 4E969
Washington, DC 20330-1000

Dr. Douglas M. Eardley
Institute for Theoretical Physics
University of California
Santa Barbara, CA 93106

Mr. John N. Entzminger
Director
DARPA/TTO
1400 Wilson Boulevard
Arlington, VA 22209-2308

Dr. Craig I. Fields
Director
DARPA
1400 Wilson Boulevard
Arlington, VA 22209-2308

Dr. Stanley M. Flatte
Physics Department
Natural Sciences II
University of California
Santa Cruz, CA 95064

Dr. Robert Foord [2]
Central Intelligence Agency
Washington, DC 20505

Dr. Norval Fortson
Department of Physics
FM-15
University of Washington
Seattle, WA 98195

Dr. Larry Gershwin
Central Intelligence Agency
Washington, DC 20505

DISTRIBUTION LIST

Dr. David Gifford
Central Intelligence Agency
Washington D.C., 20505

Dr. S. William Gouse
Sr. Vice President and General Manager
The MITRE Corporation
Mail Stop Z605
7525 Colshire Drive
McLean, VA 22102

Dr. Michael C. Gregg
Applied Physics Laboratory
1013 N.E. 40th Street
Seattle, WA 98105

LTGEN Robert D. Hammond
Commander and Program Executive Officer
U.S. Army / CSSD-ZA
Strategic Defense Command
P.O. Box 15280
Arlington, VA 22215-0150

Dr. William Happer
Department of Physics
Princeton University
Box 708
Princeton, NJ 08544

MAJGEN Jerry C. Harrison
Commander
U.S. Army Laboratory Command
2800 Powder Mill Road
Adelphi, MD 20783-1145

Dr. Robert G. Henderson
Director
JASON Program Office
The MITRE Corporation
7525 Colshire Drive, Z561
McLean, VA 22102

Mr. James V. Hirsch
Central Intelligence Agency
Washington, DC 20505

Dr. Paul Horowitz
Lyman Laboratory of Physics
Harvard University
Cambridge, MA 02138

JASON Library [5]
The MITRE Corporation
Mail Stop: W002
7525 Colshire Drive
McLean, VA 22102

Dr. O'Dean P. Judd
Chief Scientist
Strategic Defense Initiative Organization
Room 1E1083
The Pentagon
Washington, DC 20301-7100

Dr. Jonathan I. Katz
Department of Physics
Washington University
St. Louis, MO 63130

DISTRIBUTION LIST

Dr. Herbert Levine
Department of Physics
Mayer Hall/B019
University of California/San Diego
La Jolla, CA 92093

Dr. Gordon MacDonald
The MITRE Corporation
Mail Stop Z605
7525 Colshire Drive
McLean, VA 22102

Mr. Robert Madden [2]
Department of Defense
National Security Agency
ATTN: R-9 (Mr. Madden)
Ft. George G. Meade, MD 20755-6000

Mr. Charles R. Mandelbaum
U.S. Department of Energy
Code ER-32
Mail Stop: G-236
Washington, DC 20545

Mr. Arthur F. Manfredi, Jr.
OSWR
Central Intelligence Agency
Washington, DC 20505

Dr. Claire E. Max
Inst. of Geophysics & Planetary Physics
Lawrence Livermore Natl Lab
L-413
P.O. Box 808
Livermore, CA 94550

LtGen George L. Monahan, Jr.
Director/SDIO-D
Strategic Defense Initiative Organization
The Pentagon
Washington, DC 20301-7100

MGEN Thomas S. Moorman, Jr.
Director of Space and SDI Programs
Code SAF/AQS
The Pentagon
Washington, DC 20330-1000

Dr. Richard A. Muller
Lawrence Berkeley Laboratory
Building 50/Room 232
Berkeley, CA 94720

Dr. Walter H. Munk
University of California/San Diego
Scripps Institution of Oceanography
A-025
La Jolla, CA 92093

Dr. Julian C. Nall
Institute for Defense Analyses
1801 North Beauregard Street
Alexandria, VA 22311

Dr. William A. Nierenberg
Director Emeritus
Scripps Institution of Oceanography
A021
University of California/San Diego
La Jolla, CA 92093

DISTRIBUTION LIST

Dr. Robert L. Norwood [2]
Acting Director for Space
and Strategic Systems
Office of the Assistant Secretary of the Army
The Pentagon, Room 3E374
Washington, DC 20310-0103

Mr. Gordon Oehler
Central Intelligence Agency
Washington, DC 20505

Dr. Peter G. Pappas
Chief Scientist
U.S. Army Strategic Defense Command
P.O. Box 15280
Arlington, VA 22215-0280

Mr. Jay Parness
Central Intelligence Agency
Washington, DC 20505

Dr. Allen M. Peterson
Space, Telecommunications & Radioscience Lab
Department of Electrical Engineering
227 Durand Building/Stanford University
Stanford, CA 94305

MAJ Donald R. Ponikvar
Strategic Defense Command
Department of the Army
P.O. Box 15280
Arlington, VA 22215-0280

Mr. John Rausch [2]
NAVOPINTCEN Detachment, Suitland
4301 Suitland Road
Washington, DC 20390

Records Resources
The MITRE Corporation
Mailstop: W115
7525 Colshire Drive
McLean, VA 22102

Dr. Victor H. Reis
Deputy Director
DARPA
1400 Wilson Boulevard
Arlington, VA 22209-2308

Dr. Carl Romney
Center for Seismic Studies
1300 N. 17th Street, Suite 1415
Arlington, VA 22209-3871

Dr. Malvin A. Ruderman
Department of Physics
Columbia University
New York, NY 10027

Dr. Fred E. Saalfeld
Director
Office of Naval Research
800 North Quincy Street
Arlington, VA 22217-5000

DISTRIBUTION LIST

BGEN Anson Schulz
Acting Deputy Director
Strategic Defense Initiative Organization
1E1081
The Pentagon
Washington, DC 20301

Dr. Philip A. Selwyn [2]
Director
Office of Naval Technology
800 North Quincy Street
Arlington, VA 22217-5000

The Honorable Michael P.W. Stone
Secretary of the Army
Washington, DC 20310-0101

Dr. Jeremiah D. Sullivan
237C Loomis Laboratory of Physics
University of Illinois/Urbana-Champaign
1110 West Green Street
Urbana, IL 61801

Superintendent
Code 1424
Attn: Documents Librarian
Naval Postgraduate School
Monterey, CA 93943

Dr. Vigdor Teplitz
ACDA/SPSA
320 21st Street, N.W.
Room 4923
Washington, DC 20451

Dr. Sam B. Treiman
Physics Department
Princeton University
Princeton, NJ 08540

Ms. Michelle Van Cleave
Assistant Director for National Security Affairs
Office of Science and Technology Policy
New Executive Office Building
17th and Pennsylvania Avenue
Washington, DC 20506

Mr. Richard Vitali
Director of Corporate Laboratory
U.S. Army Laboratory Command
2800 Powder Mill Road
Adelphi, MD 20783-1145

Dr. Kenneth M. Watson
Marine Physical Laboratory
Scripps Institution of Oceanography
University of California/Mail Code P-001
San Diego, CA 92152

Mr. Robert Williams
Chief of Advanced Technology
DARPA
1400 Wilson Boulevard
Arlington, VA 22209-2308

RADM (Sel) Ray Witter
Director – Undersea Warfare
Space and Naval Warfare Systems Command
Code: PD-80
Department of the Navy
Washington, DC 20363-5100

DISTRIBUTION LIST

RADM Daniel J. Wolkensdorfer
Director
DASWD (OASN/RD&A)
The Pentagon
Room 5C676
Washington, DC 20350-1000

Dr. Herbert F. York
IGCC (D-018)
University of California/San Diego
La Jolla, CA 92093

Dr. Fredrik Zachariasen
California Institute of Technology
452-48
1201 East California Street
Pasadena, CA 91125

Mr. Charles A. Zraket
President and Chief Executive Officer
The MITRE Corporation
Mail Stop A265
Burlington Road
Bedford, MA 01730